

EXPERIMENTS OF CROSS-FLOW INSTABILITY IN A SWEPT-WING BOUNDARY LAYER

Zuo Sui-han*, Yang Yong*, Li Dong*

*National Key Laboratory of Science and Technology on Aerodynamic Design and Research, Northwestern Polytechnical University, Xi'an 710072, China

Keywords: *cross-flow instability; sublimation method; artificial roughness; transition control*

Abstract

Stationary cross-flow instabilities and transition pattern in the boundary layer of a 45-degree swept wing with and without 3D artificial leading edge roughness were investigated by sublimation method in two wind tunnels of Northwestern Polytechnical University. For the experiments in Low Turbulence Wind Tunnel, straight transition lines behind the minimum pressure point which are dominated by T-S instabilities appeared on the model without artificial roughness in the Reynolds number range of $5.50 \times 10^5 \sim 1.65 \times 10^6$. The traces of the most amplified stationary cross-flow waves were detected when $Re \geq 1.38 \times 10^6$, and the spacing of stripes is consistent with the results of linear stability theory. The extreme sensitivity of the stationary disturbance to leading edge roughness is verified at $Re = 1.65 \times 10^6$. With different spacing leading edge roughness applied, the most amplified waves were suppressed by the 2.5mm spacing roughness, and harmonics with half of the input wavelengths appeared when 6.0-8.0mm spacing roughness were printed. In NF-3 wind tunnel, the experiments found that as turbulence level increase, the amplification of stationary cross-flow waves are suppressed. Jagged transition line dominated by stationary cross-flow waves appeared in the upstream region of the minimum pressure point at $Re = 2.20 \times 10^6$, and the transition was delayed successfully when 1.7mm leading edge roughness was printed.

1 Introduction

Cross-flow instabilities in swept wing boundary layer were first noticed at 1952. In flight tests,

Gray [1-2] found that the transition location of a swept wing is much closer to the leading edge than that of an unswept wing. This issue was not gotten enough attention until the rise of high-speed commercial aircraft. Considering the potential engineering benefit, a large amount of investigations has been devoted to this problem over the past 20 years. The important discoveries include: environmental conditions on the appearance of stationary and traveling waves [3-4]; details of the nonlinear saturation of the dominant stationary mode and the growth of harmonics [5-8]; secondary instability causing local transition in stationary cross-flow mode dominated flows [9-11]; and extreme sensitivity of the stationary disturbance to leading edge roughness [12-13]. Another remarkable discovery is the new transition-control technique developed by Saric and co-workers at Arizona State University (ASU) [14-17]. With a proper distribution of surface roughness in the region near leading edge, the most amplified cross-flow wave can be suppressed and the transition dominated by stationary cross-flow instabilities can be controlled. Comparing with the traditional transition-control technique such as suction and thermal control [16], this method suppressing transition by the introduction of disturbance is quite novel.

The experiments conducted in two different wind tunnels of Northwestern Polytechnical University (NPU) are based on Saric's work into the investigation of cross-flow instability and the transition-control technique on swept wing. The Low Turbulence Wind Tunnel (LTWT) provides an ideal situation to investigate the stationary cross-flow instabilities, and the NF-3 Wind Tunnel offers a higher

Reynolds number to study the transition-control technique. For flow visualization, naphthalene sublimation method [18] was used. The transition pattern and traces of stationary cross-flow waves in the boundary layer of a swept wing without artificial leading edge roughness were investigated at various Reynolds numbers. Then considering the wavelengths of the most amplified waves, disturbances with various wavelengths were introduced by 3D artificial leading edge roughness, and different effects including the suppression of the most amplified waves were detected. The wind tunnels and models are described in detail in §2, experimental methods are present in §3, results of the flow visualization are given in §4, and conclusions are discussed in §5.

2 Facility

2.1 Wind Tunnel

2.1.1 Low Turbulence Wind Tunnel

LTWT in NPU (Fig. 1) is an open-circuit facility and its 2-dimensional test section is $0.4\text{m} \times 1.0\text{m} \times 2.8\text{m}$. It can be operated with a speed range of 5 to 60m/s. The turbulence level of this tunnel can be as low as 0.02 percent. This level of free-stream turbulence ensures that the cross-flow instabilities on a swept wing are dominated by stationary modes.



Fig. 1 LTWT in NPU

2.1.2 NF-3 Wind Tunnel

NF-3 Wind Tunnel in NPU (Fig. 2) is also an open-circuit facility. The 2-D test section of NF-3 Wind Tunnel is $3.0\text{m} \times 1.6\text{m} \times 8.0\text{m}$. Its

turbulence level is less than 0.05 percent and the highest speed can achieve 130m/s. It can provide sufficiently high Reynolds number to investigate the transition-control technique.



Fig. 2 NF-3 wind tunnel in NPU

2.2 Model

In order to provide an isolated situation for cross-flow instability investigation, the NLF(2)-0415 airfoil with a 45-degree sweep was chosen. There are two models used in the experiments, one has two rows of pressure taps and the other has a high polished surface. Fig. 3 is a sketch of the pressure model. This model is used to acquire the pressure distributions at different angles of attack and investigate the side wall effects in wind tunnel which cause a variation of the flow-field along span-wise direction. The root-mean-square surface roughness of the high polished model without pressure taps is $1.6\mu\text{m}$. It is used to investigate the cross-flow instability by sublimation method. Both of models have the same chord length of 0.4m and the same span length of 0.399m.

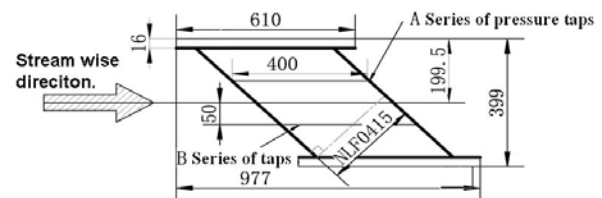


Fig. 3 Sketch of the model with two rows of pressure taps

3 Experimental Methods

3.1 Artificial Roughness

Different from the traditional artificial roughness which is used for the transition triggering, the 3-D artificial roughness in the experiment is applied for the introduction of cross-flow disturbance. The height of artificial roughness is much lower than traditional artificial roughness. Fig. 4 is the printed roughness along the leading edge of the swept wing. It was created by a special print technique—silk screen print, which is widely used in the label print. The size and spacing of roughness elements are all determined by the silk screen. In present experiments, the diameter of the roughness elements was 0.7mm and the mean height was 19.25 μ m.



Fig. 4 Distributed roughness along the leading edge of the swept wing

3.2 Sublimation Method

Sublimation technique is one of the most prevailing methods for the flow visualization. During our experiments, a naphthalene-acetone spray was used to place a white sublimating coating over the model surface. As the stationary cross-flow waves aligned along span-wise (Fig. 5) distort the velocity profiles and modify shear stresses, the characteristic that naphthalene sublimates faster in regions of high shear can not only indicate the transition location, but also offer the traces of stationary cross-flow waves in the upstream region of the transition location.

Fig. 6 is the model with entire surface sprayed in LTWT. In the sublimation figures of LTWT, the downward direction corresponds to the free-stream direction in the experiments, although there are minor directions different between each photo. The free-stream direction in the sublimation photos of NF-3 wind tunnel is from left to right. In view of the extremely

sensitivity of the stationary cross-flow waves to the surface roughness near the attachment line, an improved approach in which the naphthalene is not sprayed in the region near leading edge was applied in the experiments. The experiment results show that this improvement is necessary for the investigation of stationary cross-flow instabilities. Details will be presented in next section.

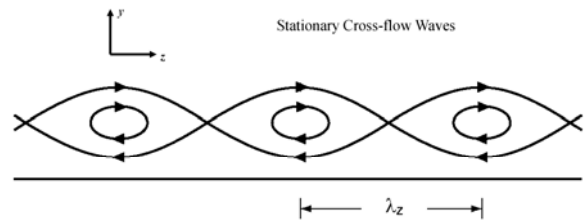


Fig. 5 Sketch of stationary cross-flow waves in the swept wing boundary layer



Fig. 6 Naphthalene sprayed on the entire upper surface of the model in LTWT

4 Results

4.1 Results in LTWT

According to the pressure measurement, the angle of attack of -4° is selected for the cross-flow instability investigation. Fig. 7 shows the surface pressure coefficient distribution for flow with $\alpha = -4^\circ$ and $Re = 1.5 \times 10^6$. The large range of the favorable pressure gradient suppresses the growth of T-S instabilities and allows the cross-flow modes to be studied in detail. There is only a little bit discrepancy between the sections at different span-wise locations. It is believed that the flow field in the central portion of the model is an approximation to an infinite swept-wing flow.

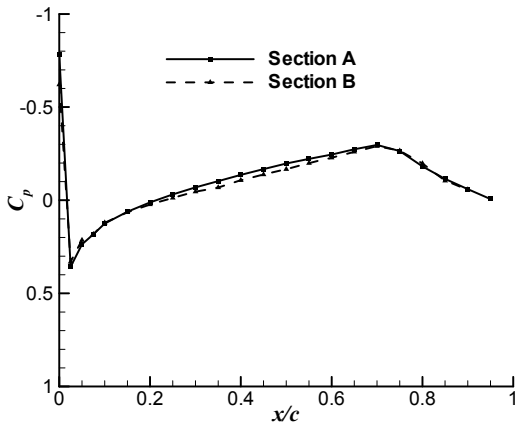


Fig. 7 Pressure coefficients at $\alpha=-4^\circ$, $Re=1.5\times 10^6$

4.1.1 Results without artificial roughness

In this part of experiments, the influences of the Reynolds number on the flow pattern were investigated. The Reynolds number ranges from 5.50×10^5 to 1.65×10^6 .

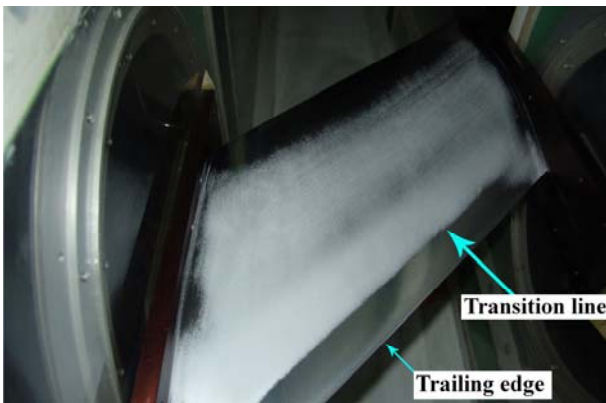


Fig. 8 Sublimation result without leading edge roughness at $Re=5.50\times 10^5$ in LTWT



Fig. 9 Sublimation result without leading edge roughness at $Re=1.10\times 10^6$ in LTWT

Fig. 8 and Fig. 9 are the results at $Re=5.50\times 10^5$ and $Re=1.10\times 10^6$. These two pictures show that the transition lines are straight-lines behind the minimum pressure point, and there are no stripes appear in the

upstream region of the transition location. This means that at these Reynolds numbers, the stationary cross-flow instabilities are not amplified enough to show themselves through the naphthalene visualization.



Fig. 10 Sublimation result without leading edge roughness at $Re=1.38\times 10^6$ in LTWT

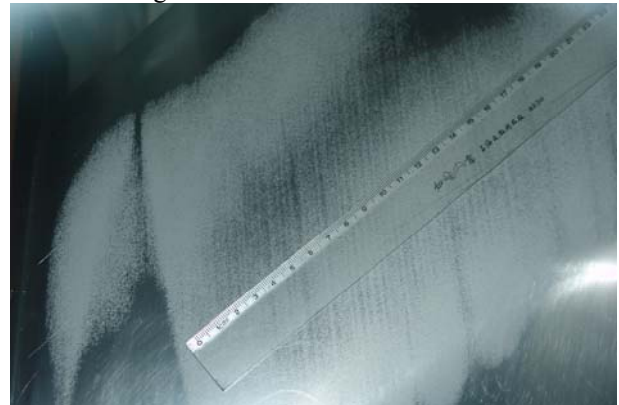


Fig. 11 Detailed photo of the stripes

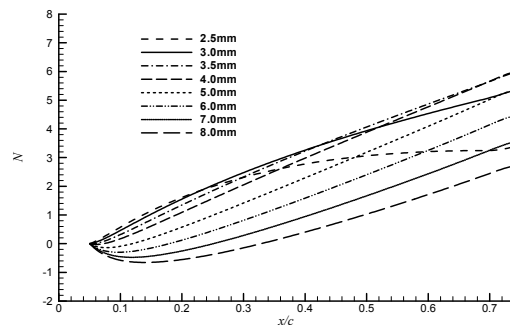


Fig. 12 N -factors based on LST at $Re=1.38\times 10^6$

Fig. 10 is the result at $Re=1.38\times 10^6$. The transition line is still a straight-line behind the minimum pressure point, but different from the results of lower Reynolds numbers, 3.5~4.0mm spacing stripes appear in the upstream region of the transition line. Fig. 11 is a detailed photo of the stripes. There are few irregular strips, which are reasonable because of the ruleless roughness on the surface of the model. These stripes show the traces of stationary cross-flow waves

developing in boundary layers. The 3.5~4.0mm spacing is thought to be the most amplified wavelength and it is consistent with the results of Linear Stability Theory (LST). Fig. 12 is the N factors computed from linear stability analysis. It can be seen that the most amplified wavelength is approximate 3.5~4.0mm.

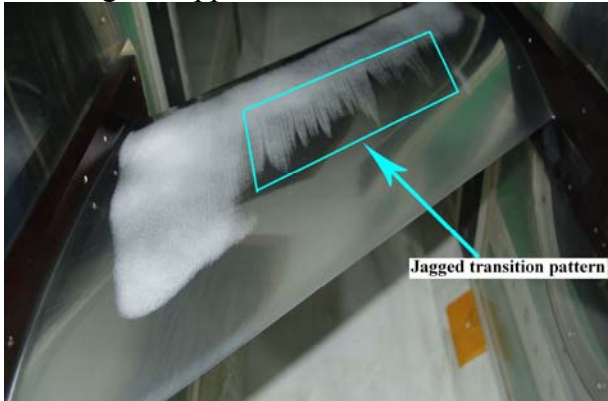


Fig. 13 Sublimation results at $Re=1.65 \times 10^6$ with entire surface sprayed in LTWT



Fig. 14 Sublimation results at $Re=1.65 \times 10^6$ with the leading edge not sprayed in LTWT

In the original experiments at $Re=1.65 \times 10^6$, the naphthalene was sprayed on the entire upper surface of the model and a jagged transition pattern (Fig. 13) was found in the upstream region of the minimum pressure point. Considering the stationary cross-flow waves are extremely sensitive to the surface roughness near the attachment line, the region near leading edge was not sprayed and the experiment was repeated. The result is showed in Fig. 14. At this time, the jagged transition pattern disappear and it shows nearly the same results as the results at $Re=1.38 \times 10^6$. This discrepancy of results from different spray methods was not found at the lower Reynolds numbers. The different results at $Re=1.65 \times 10^6$ mean that leading edge

roughness is the key in the receptivity of cross-flow instabilities. It is necessary to retain the region near leading edge not sprayed for the investigation of stationary cross-flow waves, or the naphthalene in the region near leading edge would increase the surface roughness and increase the amplitude of the instabilities.

4.1.2 Results with artificial roughness

Because the stripes on the model without artificial roughness are 3.5~4.0mm, the primary study was taken on with 3.5mm and 4.0mm spacing roughness printed at $x/c=4.5\%$. Fig. 15 is the result of 3.5mm roughness spacing at $Re=1.38 \times 10^6$. Regular 3.5mm spacing stripes were found. The transition pattern and location are the same as the nature condition (without the roughness control). Similar results appear when the 4.0mm spacing roughness were printed. Regular 4.0mm spacing stripes were found both at $Re=1.38 \times 10^6$ and $Re=1.10 \times 10^6$. Fig. 16 is the result at $Re=1.10 \times 10^6$. It is noticeable that the stripes didn't appear in the nature condition at $Re=1.10 \times 10^6$. These results indicate that, the periodic spacing roughness can influence the receptivity of stationary cross-flow instabilities and introduce a cross-flow wave with desired wavelength.

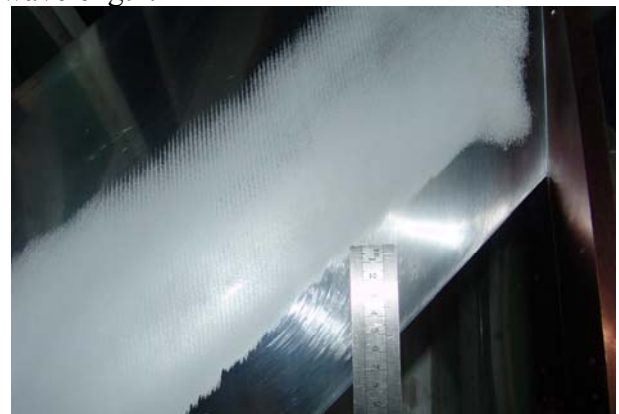


Fig. 15 Sublimation result at $Re=1.38 \times 10^6$ with 3.5mm leading edge roughness in LTWT

In order to modify the most amplified waves (3.5~4.0mm) in the boundary layer, the roughness spacing 2.5mm, 6.0mm, 7.0mm and 8.0mm were printed at $x/c=4.5\%$.

Fig. 17 is the result of 2.5mm roughness spacing at $Re=1.38 \times 10^6$. It shows that 2.5mm spacing stripes appear at $x/c=30\%-40\%$. 3.5~4.0mm spacing stripes were not detected and stripes with larger wavelengths appeared at $x/c=60\%-70\%$. All of these stripes can not be

easily identified. It is believed that the growth of 2.5mm spacing wave modifies the velocity profiles and prevents the most amplified waves from growing.



Fig. 16 Sublimation result at $Re=1.10 \times 10^6$ with 4.0mm leading edge roughness in LTWT



Fig. 17 Sublimation result at $Re=1.38 \times 10^6$ with 2.5mm leading edge roughness in LTWT



Fig. 18 Sublimation result at $Re=1.38 \times 10^6$ with 6.0mm leading edge roughness in LTWT

Fig. 18 is the result of 6.0mm roughness spacing at $Re=1.38 \times 10^6$. Fig. 19 is the result of 7.0mm and Fig. 20 is the result of 8.0mm. In these experiments, the input wavelengths were not detected but half of the input wavelengths (3.0mm, 3.5mm and 4.0mm) appeared. These half wavelengths attribute to harmonics. The

waves with 6.0mm, 7.0mm and 8.0mm wavelengths decay rapidly, but their harmonics with 3.0mm, 3.5mm and 4.0mm wavelengths grow in a large range of chord-wise. Compare with the results of 3.5mm and 4.0mm spacing roughness, the strength of the stripes induced from waves with double wavelength is weaker than those with the original control wavelength.

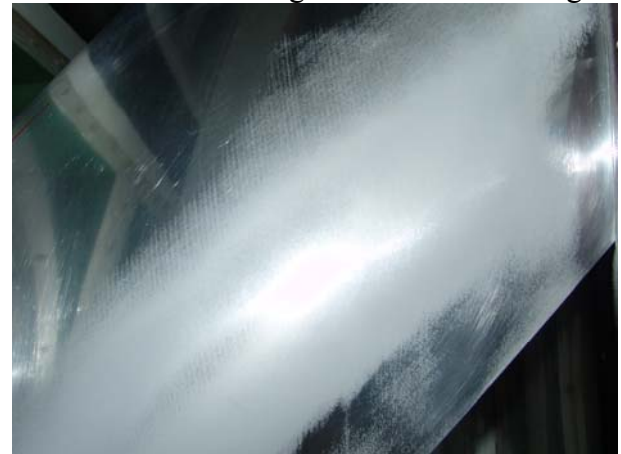


Fig. 19 Sublimation result at $Re=1.38 \times 10^6$ with 7.0mm leading edge roughness in LTWT



Fig. 20 Sublimation result at $Re=1.38 \times 10^6$ with 8.0mm leading edge roughness in LTWT

All the sublimation results in LTWT have a straight transition line behind the minimum pressure point. This means the transition is dominated by T-S instabilities. Due to the speed limitation of LTWT, transition dominated by the cross-flow instabilities was not available, and the direct transition-control effects can not be investigated. This impulse the experiments moved to NF-3 Wind Tunnel.

4.2 Results in NF-3 Wind Tunnel

Fig. 21 is the model installed in NF-3 wind tunnel. Different from the experiments in

LTWT, the model was vertical, and two side walls were fixed on the model. Due to different installation modes in two wind tunnels, the pressure coefficient distributions measured in two wind tunnels have some discrepancies. Fig. 22 is the comparison at $\alpha=-4^\circ$ and $Re=1.5\times 10^6$. It shows that the favorable pressure gradient measured in NF-3 wind tunnel is stronger, and the discrepancy between section A and section B is larger than the results gotten in LTWT. The trends of pressure distributions are the same, and the minimum pressure points are both at $x/c=70\%$. The experiments in NF-3 wind tunnel were conducted at $\alpha=-4^\circ$.

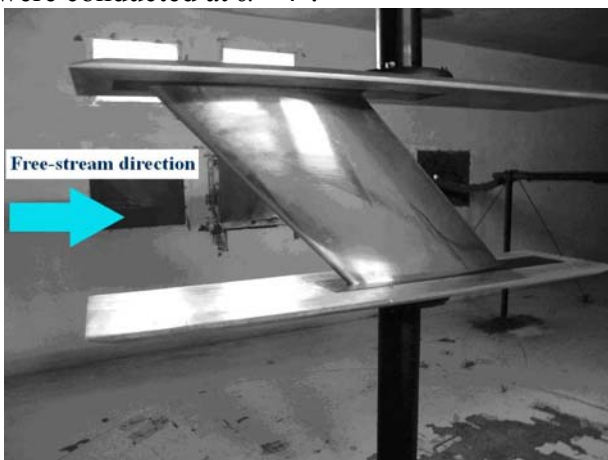


Fig. 21 Model installed in NF-3 wind tunnel

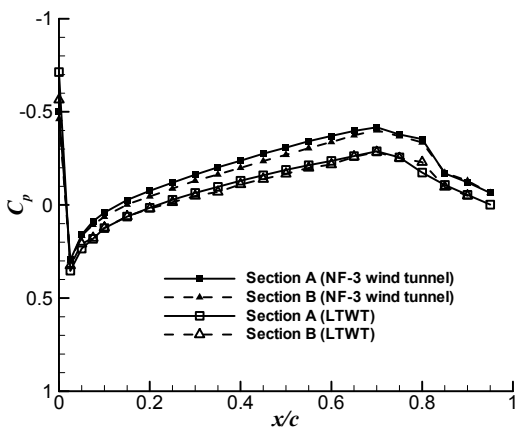


Fig. 22 Comparison of pressure coefficient distributions measured in two wind tunnels at $\alpha=-4^\circ$ and $Re=1.5\times 10^6$

Fig. 23 is the sublimation photo at $Re=1.38\times 10^6$. Straight transition line was found behind the minimum pressure point, and no stripes appeared in the upstream region of the transition location. Considering the stronger favorable pressure gradient is more unstable for the cross-flow waves [19], the disappearance of stripes is contributed to the higher turbulence

level in NF-3 wind tunnel. Owing to both the pressure distribution and turbulence level are different, the suppressive effects of the turbulence level increase to the stationary cross-flow waves need to be further investigated.



Fig. 23 Sublimation result without leading edge roughness at $Re=1.38\times 10^6$ in NF-3 wind tunnel



Fig. 24 Sublimation result without leading edge roughness at $Re=2.20\times 10^6$ in NF-3 wind tunnel



Fig.25 Detailed photo of the stripes

Fig. 24 is the sublimation result without leading edge roughness at $Re=2.20\times 10^6$. A jagged transition line appeared in the upstream region of the minimum pressure point, and 3.0-

3.3mm spacing stripes (Fig. 25) were detected. The jagged transition line means that as the Reynolds number increase, the stationary cross-flow waves are amplified enough to trigger the transition before the minimum pressure point. The variation of stripes spacing is attributed to the integrated influences of Reynolds number, pressure distribution and turbulence level.

Based on this nature wavelength at $Re=2.20\times 10^6$ is 3.0-3.3mm, 1.7mm spacing roughness were chosen as a control disturbance. Fig. 26 is the result at $Re=2.20\times 10^6$ with 1.7mm spacing roughness printed at $x/c=3.5\%$. It shows that in the region downstream of the roughness, the transition is successfully suppressed and the naphthalene retain on the model until the trailing-edge. However in the region outside of roughness effecting, the naphthalene sublimate from $x/c=80.0\%$ to the trailing-edge. For the time constraint, the optimal roughness location, spacing and height are not investigated.



Fig. 26 Sublimation result at $Re=2.20\times 10^6$ with 1.7mm leading edge roughness in NF-3 wind tunnel

5 Conclusion

Experiments of cross-flow instability in the boundary layer of a swept wing were conducted in two different Wind Tunnels. Sublimation method was used to visualize the cross-flow vortex streaks and transition pattern.

For the experimental investigations in LTWT, straight transition lines behind the minimum pressure point which are dominated by T-S instabilities appeared on the model without artificial roughness in the Reynolds number range of $5.50\times 10^5\sim 1.65\times 10^6$. When the Reynolds number exceeds 1.38×10^6 , the traces

of the most amplified stationary cross-flow waves were detected. Spacing of the traces is consistent with the results of linear stability theory. The extreme sensitivity of the stationary disturbance to leading edge roughness was verified at $Re=1.65\times 10^6$. Then different spacing leading edge roughness were applied and their effects were studied. Regular 3.5mm or 4.0mm spacing stripes appeared at $Re=1.10\times 10^6$ and $Re=1.38\times 10^6$ when 3.5mm or 4.0mm artificial roughness were printed. This means that the periodic spacing roughness can introduce the stationary cross-flow wave with desired wavelength. At $Re=1.38\times 10^6$, the 3.5~4.0mm most amplified waves were suppressed by 2.5mm spacing roughness. When the roughness spacing are 6.0mm, 7.0mm and 8.0mm, the half wavelengths resulted from harmonics were detected.

During the experimental investigations in NF-3 wind tunnel, the turbulence level is higher than LTWT, and the favorable pressure gradient is stronger at the same attack angle. Straight transition line was found and no stripes appeared at $Re=1.38\times 10^6$, which show the suppressive effects to the stationary cross-flow waves as the turbulence level increase. When the Reynolds number increased to 2.20×10^6 , the transition was dominated by stationary cross-flow waves and jagged transition line appeared in the upstream region of the minimum pressure point. Then with 1.7mm spacing roughness applied, the transition was delayed successfully. This phenomenon confirms the control method for the transition triggered by stationary cross-flow waves though artificial roughness with proper spacing which is first proposed by Saric and co-workers.

For the future works, based on a new power system fixed in LTWT, much more experiments such as the investigations of optimal control roughness and turbulence level effects will be conducted. On the other hand, a hotwire measurement under preparing will provide more detailed data for the cross-flow instabilities study.

6 Acknowledgements

This work was supported by AIRBUS Company. The authors appreciate the experts from AIRBUS Company for their constructive advice during our experiments. The invaluable help of Prof. Bai Cun-ru, Prof. Gao Yong-wei, Mr. An Long, Mr. Li Yue-li and Mr. Luo Kai is gratefully acknowledged.

References

- [1] Gray WE. The effect of wing sweep on laminar flow. *RAE TM Aero* 256, 1952.
- [2] Gray WE. The nature of the boundary layer flow at the nose of a swept wing. *RAE TM Aero* 256, 1952.
- [3] Deyhle H and Bippes H. Disturbance growth in an unstable three-dimensional boundary layer and its dependence on initial conditions. *J. Fluid Mech.*, No. 316, pp 73-113, 1996.
- [4] Bippes H. Basic experiments on transition in three-dimensional boundary layers dominated by crossflow instability. *Progress in Aerospace Sciences*, Vol. 35, No. 4, pp 363-412, 1999.
- [5] Bippes H and Nitschke-Kowsky P. Experimental study of instability modes in a three-dimensional boundary layer. *AIAA J.*, Vol. 28, No. 10, pp 1758-1763, 1990.
- [6] Dagenhart J R, Saric W S, Mousseux M C and Stack J P. Crossflow vortex instability and transition on a 45-degree swept wing. *AIAA-89-1892*.
- [7] Radeztsky Jr R H, Reibert M S and Saric W S. Development of stationary crossflow vortices on a swept wing. *AIAA-94-2373*.
- [8] Reibert M S, Saric W S, Carrillo R B Jr and Chapman K L. Experiments in nonlinear saturation of stationary crossflow vortices in a swept-wing boundary layer. *AIAA-96-0184*.
- [9] Kohama Y, Saric W S and Hoos J A. A high frequency, secondary instability of crossflow vortices that leads to transition. *Proc. R. Aeronaut. Soc. Conf. on Boundary-Layer Transition and Control*, Cambridge, UK, 4.1-4.13, 1991.
- [10] Kohama Y, Onodera T and Egami Y. Design and control of crossflow instability field. *Proc. IUTAM Symp. On Nonlinear Instability and Transition in Three-Dimensional Boundary Layers*, Manchester, UK (ed. P. W. Duck and P. Hall), pp 147-156, 1996.
- [11] White E B and Saric W S. Secondary instability of crossflow vortices. *J. Fluid Mech.*, No. 525, pp 275-308, 2005.
- [12] Radeztsky Jr R H, Reibert M S, Saric W S and Takagi S. Effect of micro-sized roughness on transition in swept-wing flows. *AIAA-93-0076*.
- [13] Radeztsky Jr R H, Reibert M S and Saric W S. Effect of isolated micron-sized roughness on transition in swept-wing flows. *AIAA J.*, Vol. 37, No. 11, pp 1370-1377, 1999.
- [14] Saric W S, Carillo R B and Reibert M S. Leading-edge roughness as a transition control mechanism. *AIAA-98-0781*.
- [15] White E B and Saric W S. Application of variable leading-edge roughness for transition control on swept wings. *AIAA-2000-0283*.
- [16] Saric W S and Reed H L. Toward practical laminar flow control—remaining challenges. *AIAA-2004-2311*.
- [17] Martin M L, Carpenter A L and Saric W S. Swept-wing laminar flow control studies using Cessna O-2A test aircraft. *AIAA-2008-1636*.
- [18] Dagenhart J R and Saric W S. Crossflow stability and transition experiments in swept-wing flow. *NASA/TP-1999-209344*.
- [19] Haynes T S. *Nonlinear stability and saturation of crossflow vortices in swept-wing boundary layers*. PhD thesis, Arizona State University, 1996.

Copyright Statement

The authors confirm that they, and/or their company or organization, hold copyright on all of the original material included in this paper. The authors also confirm that they have obtained permission, from the copyright holder of any third party material included in this paper, to publish it as part of their paper. The authors confirm that they give permission, or have obtained permission from the copyright holder of this paper, for the publication and distribution of this paper as part of the ICAS2010 proceedings or as individual off-prints from the proceedings.